# Mechanism of Partial Flame Propagation and Extinction in a Strong Gravitational Field

Kirill A. Kazakov
*Moscow State University, 119991 Moscow, Russian Federation*
(Received 19 July 2015; published 23 December 2015)

A theory of partial flame propagation driven by the gravitational field is developed. Using the on-shell approach, equations for the gas velocity distributions and the front shape of a steady flame are obtained and solved numerically. It is found that the solutions describing upward flame propagation come in pairs having close propagation speeds, and that the effect of strong gravity is to reverse the burnt gas velocity profile generated by the flame. On the basis of these results, a complete explanation is given of the intricate observed behavior of flames near the limits of inflammability, including the dependence of the inflammability range on the size of the combustion domain, the large distances of partial flame propagation, and the progression of flame extinction.

DOI: 10.1103/PhysRevLett.115.264501 PACS numbers: 47.70.Pq, 47.20.-k, 47.32.-y, 82.33.Vx

As is well known, the gravitational field has a profound effect on the dynamics of reaction waves, be it flame propagation in gaseous mixtures under terrestrial conditions [1] or thermonuclear waves in supernovae [2]. Gravity's impact on deflagrations is important practically at all scales, from the laboratory explosions in tubes to their industrial applications. But it is especially pronounced near the inflammability limits—the end points of the range of fuel concentrations over which a given mixture is able to sustain laminar flame propagation. As these are of special interest with regard to combustion safety, much effort has been spent on their experimental and theoretical study [3–8].

The inflammability limits are measured in vertical tubes closed at the upper end, sufficiently wide to make negligible heat loss to the tube walls, ignition being effected at the bottom, open, end (a standard tube is 5.1 cm in diameter and 1.8 m long [3]). In view of the practical significance of methane-air and propane-air flames, elaborate precision measurements of their limit properties have been performed in tubes of different diameters [3–6]. The studied flames were characterized by different fresh-to-burnt gas density ratios $\theta = 4.7$ to $\theta = 5.3$, and had different burning rates and molar-mass relations between fuel and oxidizer. Despite these distinctions, a great deal of similarity in the limit flame behavior has been established, which can be summarized as follows. (i) Before extinction, flames can propagate steadily over distances largely exceeding the flame size, at least in tubes with diameter up to 10 cm. The onset of extinction is simultaneous with a slight increase in the flame speed. (ii) The inflammability range narrows in wider tubes; that is, the minimal burning rate required to propagate the flame increases with the tube diameter. (iii) The propagation speed of the limit flames in a tube of given diameter coincides, within the experimental error, with the speed of an air bubble rising in the same tube filled with water. In particular, it is independent of the fuel type. (iv) Reactants flow into the rising flame, but only around the hot postflame structure that continues to rise with the same speed after the flame extinction. During extinction, the flame center vanishes first, followed rapidly by the edges.

Taken together, these observations make the nature of partial flame propagation and its extinction quite a riddle. On the one hand, the apparent flame steadiness before extinction means that the characteristic time of partial flame propagation is much larger than the transit time of gas through the region occupied by the flame (transition domain in what follows). On the other hand, the final stage of the process is much more rapid, according to (iv). The latter would take place if the extinction process were buoyancy driven, as is also suggested by observation (iii), but in that case the flame ought to extinguish right upon entering the steady regime, that is, a few tube diameters above the ignition point, in contradiction to the first part of (i). The second observation of (i) is confusing on its own, as the flame which is about to extinguish would rather be expected to decelerate. Next, heat losses to the walls, which are generally an important factor of flame extinction, cannot drive the process under consideration because their relative value diminishes as the tube diameter increases, and so they would produce a trend opposite to (ii). In fact, it is known that the heat losses are negligible for axisymmetric flames propagating in tubes with diameter $\gtrsim 2$ cm. Neither can extinction be effected by the flame stretch [6,7]. In the case of methane-air flames, for instance, the flame stretch increases the burning rate at the flame center [9], thus leading to contradiction with (iv). This mechanism is also unable to explain (ii), because it would produce opposite trends in mixtures with light and heavy deficient components (such as lean methane-air and propane-air mixtures, respectively), contrary to what is observed.

The extinction problem will be resolved below using the recently developed on-shell flame description [10,11]; the

 

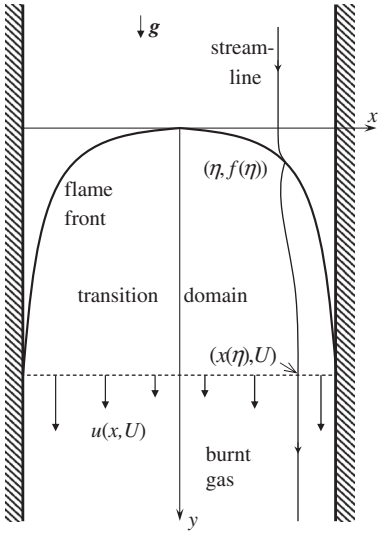


FIG. 1. Schematics of upward flame propagation in the case $g \gg 1$. Vertical arrows attached to the lower boundary (dashed line) of the transition domain $y \in (0, U)$ depict the burnt gas velocity profile generated by the flame under strong gravity.

intricacy of properties (i)–(iv) will be shown to be due to a rather nontrivial structure of the spectrum of flame propagation regimes under strong gravity.

It is quite clear that such a qualitative feature as the extinction mechanism is common for two- and three-dimensional flames. We therefore consider the mathematically simpler two-dimensional configuration, wherein the flame propagates in an initially quiescent gaseous mixture filling a vertical channel of width equal to the tube diameter; see Fig. 1. Although flame extinction is in itself an unsteady phenomenon, the experimental evidence stated in (i) suggests that the conditions for its occurrence can be inferred from the properties of the steady regime. We therefore choose the reference frame attached to the steady flame, with the origin at its tip, denoting $x$ the horizonal coordinate and $y$ the coordinate directed downward along the channel centerline. Lengths will be measured in units of the channel half-width, $d/2$, whereas the gas velocity components $(w, u)$, in units of the planar flame speed relative to fresh gas $U_f$. As the latter is much smaller than the sound speed, the gas flow can be treated as incompressible. Also, since the heat losses are not important for the studied phenomenon, the gas density can be assumed constant both upstream and downstream of the flame front, $\theta$ denoting the density ratio. Then the gas-velocity distributions along the flame front, considered as a gas dynamic discontinuity at $y = f(x)$, satisfy the following complex integro-differential equation [10], which is an exact consequence of the fundamental gas dynamic equations for ideal flow:

$$2\omega'_- + (1 + i\hat{\mathcal{H}})\left\{[\omega]' - \frac{N v_+^n \sigma_+ \omega_+}{v_+^2}\right\} = 0. \qquad (1)$$

Here, $\omega = u + iw$ is the complex velocity, $[\omega] = \omega_+ - \omega_-$ its jump across the front, prime denotes $x$ differentiation, the subscript $-$ $(+)$ restriction to the front of a function defined upstream (downstream) of the front, e.g., $w_-(x) = w(x, f(x) - 0)$, $N = \sqrt{1 + f'^2}$, $v^n$ is the normal gas velocity, $\sigma = \partial u/\partial x - \partial w/\partial y$ the vorticity, and, finally, the $\hat{\mathcal{H}}$ operator is defined on continuous functions $a(x)$ with zero mean across the channel as

$$(\hat{\mathcal{H}}a)(x) = \frac{1 + if'(x)}{2} \fint_{-1}^{+1} d\eta a(\eta) \times \cot\left\{\frac{\pi}{2}\{\eta - x + i[f(\eta) - f(x)]\}\right\},$$

where the slash denotes the principal value of the integral. Equation (1) is to be complemented by the evolution equation, which defines the local burning rate. In terms of the fresh gas velocity at the front, it reads

$$u_- - f' w_- = N - \mathcal{L}(v^\tau)', \qquad (2)$$

where $v^\tau = (w_- + f' u_-)/N$ is the tangential to the front component of the gas velocity. The last term on the right-hand side of Eq. (2) describes the stretch effect, $\mathcal{L}$ denoting the Markstein length. Effects due to the front curvature can be safely omitted in the case under consideration, because the radius of the flame front curvature is much larger than the front thickness. Calculations show that for methane-air flames in the standard flammability tube, for instance, the relative value of the curvature contribution is less than 1%.

In its exact form, the system of Eqs. (1) and (2) is very complicated. Fortunately, it highly simplifies for flames with elongated fronts; such are the limit flames according to the experiment. Transformations quite similar to those performed in Ref. [11] for flames in horizontal channels yield two real equations that can be conveniently written taking $f$ as an independent variable:

$$\frac{d}{df}\left[\frac{du_-}{df}(1 + \alpha x) - \frac{\alpha g x}{u_-}\right] + \frac{\alpha}{u_-^2}\left(u_- \frac{du_-}{df} - g\right)(w_- - \alpha) = 0, \qquad (3)$$

$$w_- = (1 - x)\frac{du_-}{df}, \qquad (4)$$

where $g$ is the gravity acceleration, $\alpha \equiv \theta - 1$, and we consider the right half of the channel, $x > 0$. These ordinary differential equations are to be integrated together with Eq. (2) under the initial conditions [11]

$$u_-(0) = U, \qquad \frac{du_-(0)}{df} = \frac{\alpha}{2}, \qquad (5)$$

where $U$ is the flame propagation speed in the laboratory frame.

Numerical scrutiny of the system shows that there are two families of solutions corresponding to two disjoint continua of $U$'s, just as for horizontal flame propagation. As in the latter case, solutions corresponding to the lower (higher) $U$ will be called type I (type II) flames. Physical solutions are identified as those satisfying

$$\int_0^1 d\eta N u(x(\eta),U) = \frac{u_1^2+U^2}{2} + \frac{\alpha g}{\theta}\int_0^1 d\eta[f(\eta)-U] + \alpha,$$

where $(x(\eta),U)$ is the intersection of the line $y=U$ with the streamline that crosses the front at $(\eta,f(\eta))$, Fig. 1, $u_1$ the fresh gas velocity at the front end point $(1,U)$, and

$$u(x(\eta),U) = \{\theta u_1^2 - \alpha u_-^2(\eta) + 2\alpha g[f(\eta)-U]\}^{1/2} \qquad (6)$$

the burnt gas velocity at the lower boundary of the transition domain. This condition expresses conservation of the flow momentum through the transition domain.

An important and quite unexpected feature revealed by the numerical analysis is that in the region of parameters $\theta, U_f, \mathcal{L}$ typical of limit flames, type I solutions come in pairs having close $U$'s. Thus, for a flame with $\theta = 4.7$, $U_f = 6.57$ cm/s, and $\mathcal{L} = -0.62$ mm in the standard flammability tube, the two eigenvalues are 3.38 and 3.75. There is also one type II solution which, however, has a too high speed $U = 21.4$ to be relevant to the inflammability issue; if stable, it can presumably be realized by means of a sufficiently strong ignition source. For brevity, type I solutions with the lower (higher) speed will be referred to as type Ia (type Ib).

The following circumstance is the key to explaining the phenomenon of flame extinction. In the absence of gravity, the gas flow induced by the flame is normally such that the combustion products leaving the transition domain move faster near the channel centerline than near the walls. This is because, under the given overall pressure drop through the transition domain, the velocity gain is larger for smaller gas density, so that the gas elements burned near the flame leading edge are accelerated stronger than those traversing this domain in its upstream part. The effect of gravity [the term $2\alpha g[f(\eta)-U]$ in Eq. (6)] is opposite: the gas elements flowing closer to the centerline are decelerated more strongly. Numerical integration of the above system shows that near the inflammability limits, the latter effect predominates over the former: under strong gravity ($g \gg 1$), the function $u(x(\eta),U) \equiv u(\eta)$ turns out to increase with $\eta$; see Fig. 2. Numerical analysis reveals, furthermore, that type Ib solutions are singular at sufficiently small $U_f$ (that is, sufficiently large $g$). Namely, as the normal flame speed decreases to some critical $U_f$ (dependent on $\theta$), $u(\eta)$ vanishes at the channel centerline ($\eta = 0$). For still smaller $U_f$, the root $\eta_0$ of the function $u(\eta)$ shifts from the centerline towards the wall, while $u(\eta)$ becomes formally imaginary at $\eta < \eta_0$; that is, the steady regime of the flame propagation ceases to exist. Nullification of the gas velocity over a finite region behind the flame means physically that the burnt gas stops to flow out of the corresponding region of the flame front. This is, of course, impossible in a truly steady regime with a finite burning rate, but this also means that if, for some reason, a flame configuration is instantly formed with the gas velocity distribution along the front and the front shape characteristic of a supercritical type Ib solution, it will not exist longer than the transit time of burnt gas from the front to the region of vanishing velocity. In other words, the pressure distribution in this case is such that the gas burning near the channel centerline is strongly pushed upwards downstream of the front. One possible outcome of this situation is a continued essentially unsteady flame propagation, the other possible outcome is its extinction.

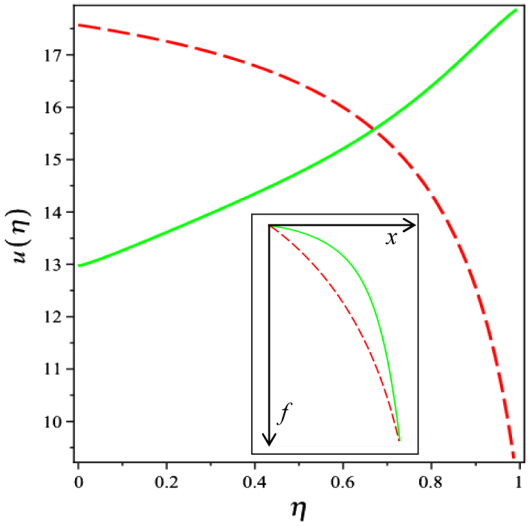


FIG. 2 (color online). Burnt gas velocity distributions at the lower boundary of the transition domain for a type I flame in strong gravity (solid line, $g = 51$), and a flame anchored in a fast stream (dashed line, $g = 0$). Inset: The corresponding front shapes. $d = 5.1$ cm, $\theta = 4$, $\mathcal{L} = -0.1$.

Figure 3 is a phase diagram representing critical conditions in the $U_f - \theta$ plane for different $d$ and $\mathcal{L}$. Stable (subcritical) type Ib regimes belong to the region on the right of the critical curve with the given $d, \mathcal{L}$. The values of $U_f, \mathcal{L}$ for near-limit flames are not easy to determine accurately, but quite remarkably, the propagation speed of type Ib flames turns out to change very little along the critical curves when expressed in cm/s. In the case of $d = 5.1$ cm and $\mathcal{L} = -0.62$ mm, for example, $U$ belongs to the interval $24.65 \pm 0.1$ cm/s as $\theta$ varies from 4 to 5, and $U_f$, respectively, from 6.3 to 5.3 cm/s, whereas a threefold reduction of $\mathcal{L}$ gives rise to only a 5% change in $U$.

The whole picture of partial flame propagation can now be described as follows. Ignition by means of a weak

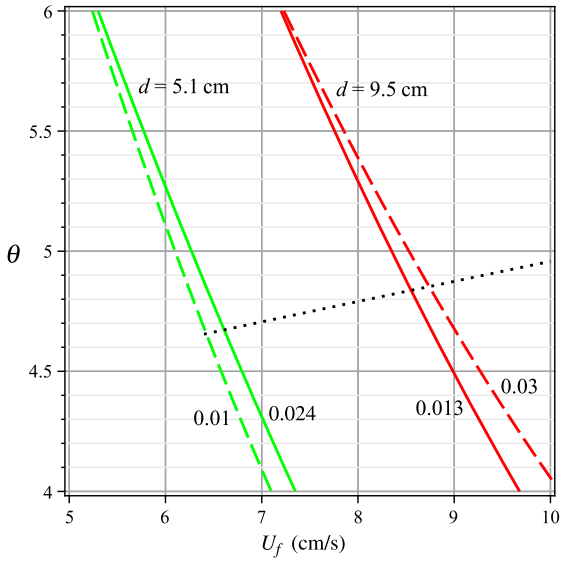


FIG. 3 (color online). Critical conditions for flame extinction in tubes of diameters 5.1 and 9.5 cm. Solid lines correspond to $\mathcal{L} = -0.62$ mm, as given in Ref. [9] for methane-air flame with the equivalence ratio 0.55. The dotted line is the phase locus of lean methane-air flames, drawn using the same source. Also shown are the critical curves for significantly different $\mathcal{L}$ (dashed lines). The numbers near the lines are moduli of the respective dimensionless Markstein lengths.

energy source results in a steady flame with the lowest propagation speed, that is, a type Ia flame. The flame travels as such for some distance, but sooner or later it goes over to the faster type Ib regime. (Numerical analysis shows that under the critical conditions, the bulk viscous forces alone are incapable of transforming the burnt gas flow into the state of thermodynamic equilibrium—a homogeneous flow. The type Ia flame thus turns out to be metastable: it acquires a burnt gas "tail" in a state of incomplete equilibrium, of length $\gg d$ equal to the distance at which the boundary layer thickness becomes $\sim d$.) If the latter is subcritical, the flame continues to propagate with a slightly increased speed, which is thus the flame speed that will be measured in a sufficiently long tube. On the other hand, if the flame is supercritical, then as was already mentioned, flame extinction following a short transient is one of the two possibilities for flame evolution after the loss of stationarity. It is to be expected for flames that are less energetic (leaner), hence, less resistant to the flow perturbation taking place near the flame center. Since the critical curves in Fig. 3 shift to the leaner side as the tube diameter decreases, this outcome is favored in sufficiently narrow tubes, and as the experiments show, it is actually observed in tubes with $d \lesssim 10$ cm. In wider tubes, on the other hand, the flame might continue to propagate, but in an essentially unsteady regime, e.g., break into cells.

Characteristics (i)–(iv) of the observed flame behavior are readily understood in this picture. Figure 3 demonstrates that the critical normal flame speed increases with the tube diameter; that is, the inflammability range narrows in wider tubes, in agreement with the observation (ii). The existence of the type Ia regime under critical conditions makes possible comparatively long steady flame propagation before extinction [the first part of (i)], whereas transition to the slightly faster short-lived type Ib flame configuration accounts for the rest of (i). It was already discussed how specifics of the type Ib solution explain the fact that extinction begins at the flame center [the last observation in (iv)]. Turning finally to (iii), it should now be clear that the same property of type Ib solutions establishes a direct link between limit flames and bubbles: the flow stoppage developing from the flame center towards the walls makes the two structures alike. Together with the fact already mentioned that the flame propagation speed changes very little along the critical curves, this fully accounts for (iii). A quantitative comparison of the theory with experiment is given in Table I.

TABLE I. Methane-air flames in the lean extinction limit in tubes of two different diameters. $\theta$ and $U_f$ correspond to intersections of the critical curves in Fig. 3 with the dotted line. $U_{\mathrm{exp}}$ is the measured flame propagation speed [4], $U_{\mathrm{Ia}}$ and $U_{\mathrm{Ib}}$ its values as given by the type Ia and type Ib solutions. Experimental accuracy is 5%–7%; the error of calculations is about 10%.

| $d$ (cm) | $\theta$ | $U_f$ (cm/s) | $U_{\mathrm{exp}}$ (cm/s) | $U_{\mathrm{Ia}}$ (cm/s) | $U_{\mathrm{Ib}}$ (cm/s) |
|---|---|---|---|---|---|
| 5.1 | 4.7 | 6.57 | 23.5 | 22.2 | 24.6 |
| 9.5 | 4.8 | 8.60 | 33.1 | 30.2 | 33.1 |

Regarding the similarity of limit flames with bubbles, its transitory nature should be emphasized. Although the burnt gas slow-down takes place in both Ia and Ib regimes, the gas velocity in type Ia solutions remains large compared to $\theta U_f$ everywhere in the channel cross section at $y = U$, so that no analogy with bubbles exists. This analogy emerges only at the latest stage of flame evolution following transition to a critical type Ib regime, when the burnt gas stops to flow along the centerline, resulting in the local flame extinction which then rapidly spreads out along the front. In other words, a steady flame never behaves like a bubble, but so does the hot postflame structure, that is the type Ib flame remnant.

The fact that the bubble analogy holds only under the critical conditions has another interesting implication. The bubble speed is known to scale with $g, d$ as $U \sim \sqrt{gd}$. At the same time, it is not difficult to see that $g$ cannot be eliminated from Eqs. (3) and (4) by rescaling $u_- \to \sqrt{g}u_-$, $f' \to \sqrt{g}f'$. This means that the dependence of $U$ on $g$ is more complicated in general. Thus, the scaling $U \sim \sqrt{gd}$ holds only in the critical solutions, and as the numerical analysis shows, it does so only approximately.

This study was partially supported by RFBR, research project No. 13-02-91054 a.

[1] Ya. B. Zel'dovich *et al.*, *Mathematical Theory of Combustion and Explosions* (Plenum Press, New York, 1985).
[2] W. Hillebrandt and J. C. Niemeyer, Annu. Rev. Astron. Astrophys. **38**, 191 (2000).
[3] H. F. Coward and G. W. Jones, U.S. Bureau of Mines Bull. 503 (1952); M. G. Zabetakis, U.S. Bureau of Mines Bull. 627 (1965).
[4] A. Levy, Proc. R. Soc. A **283**, 134 (1965).
[5] J. Jarosinski, R. A. Strehlow, and A. Azarbarzin, Symp. (Int.) Combust. **19**, 1549 (1982).
[6] E. von Lavante and R. A. Strehlow, Combust. Flame **49**, 123 (1983).
[7] J. Buckmaster and D. Mikolaitis, Combust. Flame **45**, 109 (1982).
[8] L. A. Lovachev, Combust. Flame **17**, 275 (1971); B. Bregeon, A. S. Gordon, and F. A. Williams, Combust. Flame **33**, 33 (1978); P. Pelce, J. Phys. (Paris) **46**, 503 (1985).
[9] D. Bradley, P. H. Gaskell, and X. J. Gu, Combust. Flame **104**, 176 (1996).
[10] K. A. Kazakov, Phys. Rev. Lett. **94**, 094501 (2005); Phys. Fluids **17**, 032107 (2005).
[11] K. A. Kazakov, Phys. Fluids **24**, 022108 (2012).